



## Research Article

# Remote sensing and geographic information system (GIS)-based high-resolution mapping of potential groundwater recharge zones on the hard rock terrains of the Cameroon volcanic line (CVL)

Mbohliou Tchawe Yossa<sup>1,2,4</sup>  · Anatole E. Djieto Lordon<sup>1</sup> · Christopher M. Agyingi<sup>1</sup> · Junior Agbor-Taku<sup>4,6</sup> · Yves N. Shandini<sup>2,3</sup> · Crayton Enga Bessong<sup>5</sup>

Received: 24 June 2022 / Accepted: 30 November 2022

Published online: 17 December 2022

© The Author(s) 2022 [OPEN](#)

## Abstract

Groundwater is the major water reserve in the present context of global warming-related droughts that appear to be more intense in hard rock terrains. The use of Geographical Information Systems (GIS) and Remote Sensing (RS) technologies are increasingly beneficial to groundwater research, by allowing for low cost and larger-scale high-resolution mapping compared to conventional hydrogeological exploration methods. This study aimed at developing a high-resolution map of potential groundwater recharge ( $GWR_{pot}$ ) zones for the drought-stricken Banka hard rock terrain, straddling the Cameroon Volcanic Line (CVL). Shuttle Radar Tomography Mission (SRTM)-30m and Landsat 8 satellite images constituted the main data source that was ground-truthed through field mapping and used to produce various thematic GIS layers: geology slope, aspect, land use & land cover, drainage density and lineament density of spatial resolution 16m x 16m. The layers were each attributed a fixed score and weight to groundwater recharge, computed using Multi-Influencing Factor (MIF) and Analytical Hierarchy Process of Multi-Criteria Decision Analysis (AHP-MCDA) techniques. Lastly, a Weighted Overlay Analysis was done using the layers to produce the  $GWR_{pot}$  zones for the study area. The resulting map shows that 60% of the study area, covering the south, west-northwest and the north-northeast portions of the map have moderate to very high recharge potentials. This result is particularly useful for groundwater targeting in the area and demonstrates the effectiveness of the method in hard rock terrains where traditional methods have been less efficient in properly delineating groundwater recharge zones.

## Article highlights

- Groundwater is generally the safest and most reliable source of water in water scarce environments, and forms when surface water goes into the ground.
- More areas where water can enter the ground means more chances of getting enough groundwater. Conventional ways of knowing these areas are time consuming and costly, whereas RS and GIS-based methods are less costly and use lesser time.
- We used the RS, GIS, high-resolution field mapping and statistical methods of blending several factors to produce the potential groundwater recharge zones on a part of the hardrocks of the CVL, that shows 60% of the study area, covering the south, west-northwest and the north-northeast portions of the area have moderate to very high recharge potentials.

✉ Mbohliou Tchawe Yossa, [yossa.brice@hotmail.com](mailto:yossa.brice@hotmail.com) | <sup>1</sup>Department of Geology, University of Buea, Buea, Cameroon. <sup>2</sup>GeoXplore, Douala, Cameroon. <sup>3</sup>Applied Sciences and Technology Laboratory, Institute of Technology, University of Douala, Douala, Cameroon. <sup>4</sup>Technical School of Mines, National Technological Institute of Mining and Hydrocarbons, Mongomo, Equatorial Guinea. <sup>5</sup>Department of Earth sciences, University of Gothenburg, Göteborg, Sweden. <sup>6</sup>Institute of Geological and Mining Research, Yaoundé, Cameroon.



SN Applied Sciences

(2023) 5:30

| <https://doi.org/10.1007/s42452-022-05248-w>

SN Applied Sciences  
A **SPRINGER NATURE** journal

**Keywords** Groundwater recharge · Remote sensing · Geographic information system · Multi-Influencing factor technique · Analytical hierarchy process · Cameroon volcanic line

## 1 Introduction

Banka subdivision is located within the hardrocks that make up the highlands and steep slopes of the Cameroon Volcanic Line (CVL), Western Cameroon. The locality is prone to having most of its precipitation becoming surface or near-surface run-off, which associates to the recently recorded droughts to lead to chronic water shortages in the area. Groundwater is considered the main solution to the water shortage in the area, although the resource is barely exploited. The first pre-requisite for aquifer formation is precipitation percolation to recharge underground formations [1–3]. Therefore, exploration and sustainable management of aquifers demands a good mapping of groundwater recharge zones. Groundwater recharge is effective only when water leaves the unsaturated zone to the saturated zone [4, 5]. Lineaments, drainage patterns, geology, slope, Land use & Land cover (LULC) and climate are some of the factors that affect groundwater recharge [6, 7]. Hence understanding the groundwater recharge potential ( $GWR_{pot}$ ) of an area requires a careful consideration of these factors [2]. Though done in several parts of the world, such studies have rarely been done in Cameroon, and hence very little is scientifically documented on the groundwater recharge potential of most hardrock regions in Cameroon. Therefore, this piece of work starts shedding light to build the scientific body of knowledge in this branch of studies nation-wide. The study is unique in that it uses high spatial resolution geologic data (1 sample every 400m) in the mix of factors, as compared to the regional geologic data mostly used in the majority of studies [1–3, 6, 7] with similar methodologies. The reason for using the detailed geologic map is that regional geologic maps available shows only one rock type in the study area, and will hence not produce an adequate GRWpot map in the study area at this scale since geology is a primordial factor in groundwater recharge zone assessment. The detailed geologic map we produced in this study showed the presence of more than three rock types

in the study area, having very different brittle characteristics and hence different recharge potentials. Moreover, the study is self-sponsored and is intended to serve as a model cell for the generation of similar neighbor cells (using bigger funds) which will eventually be part of a regional high-resolution GRWpot map.

[2, 8 and 9] stipulate that the conventional way of calculating  $GWR_{pot}$  is through soil moisture modeling from hydrogeological field investigations. Nevertheless, these in-situ investigations are costly and time consuming at catchment level. Remote sensing techniques together with GIS provide a faster and more cost-effective alternative to estimate  $GWR_{pot}$ . The method consists in mapping various factors that affect  $GWR_{pot}$  and integrating them to produce a  $GWR_{pot}$  map [e.g. 3, 6, 10, 11, 12, 13, 14, 15, 16]. The integration is done by multiplying each individual raster by their relative weights, which is a measure of their impact on the  $GWR_{pot}$  of the area. The attribution of weights is subjective and is based either on literature values [e.g. 11, 17, and 18] or on expert knowledge [13, 15, and 19]. However, the stronger the influence of one factor on others, the larger its importance relative to the others and therefore the larger its relative weight [1, 4, 6, 20–22]. This is known as the Multi-Influencing Factor technique (MIF) [2]. Another statistically concise expert-guided way of assigning weight is by using the Analytical Hierarchy process proposed by [23], which ranks the factors after a pair-wise comparison that evaluated relative importance of factors to groundwater recharge.

This study focuses on mapping the potential groundwater recharge zones within Banka subdivision, using RS and GIS techniques. Six factors that influence groundwater recharge including geology (GE), lineament density (LD), drainage density (DD), slope (SL), aspect (AS) and LULC alongside their weights were used to develop a high-resolution map showing groundwater recharge potential zones. Aspect has been scarcely used in groundwater studies, despite it being an important factor

that can give an idea about the surfaces that are exposed to solar radiation and hence an estimate of evapotranspiration [2]. Since the study area is a hard rock terrain, this map will facilitate groundwater exploration by zooming-in to the most prolific areas where to concentrate more advanced field investigation techniques. The fact these kinds of studies have not been done in this part of the country according the authors' knowledge will make this work serve as a base for subsequent studies in this light.

The paper is structured such that we give a brief background and objectives of the study in the introduction, followed in Sect. 2 by an idea of the location, geographic and geologic setting of the study area. The next section describes the material and methods used to attain the set objectives, while Sect. 4 presents and discusses the results that we got. We finally give our conclusions and recommendations for better works in the last section.

## 2 Location and geology

This study area is located administratively in the Banka subdivision, West Region of Cameroon. It forms a part of the Western Highlands of the Cameroon Volcanic Line (CVL; Fig. 1a-b), and constitutes the highlands, surrounded to the north and NW by the Bambouto Caldera, to the east by the Bamoun plateau and Noun plain, and to the SE by Mounts Bana and Bangou [24, 25]. The landscape is highly undulatory, with steep slopes and occasional deep passes. The nation-wide geologic map of Cameroon (Fig. 1a) shows that basalts and gneisses dominate the area [26]. The drainage network is dendritic and composed of two major (up to 10m wide in some places) watercourses that cross the subdivision (Fig. 1b, c), fed by numerous small springs and streams, sourced from hillsides.

The climate is of Guinean Sudano type with an altitude that favors abundant precipitations reaching an annual average of 1500 mm [27, 28]. The rains used to be concentrated between the

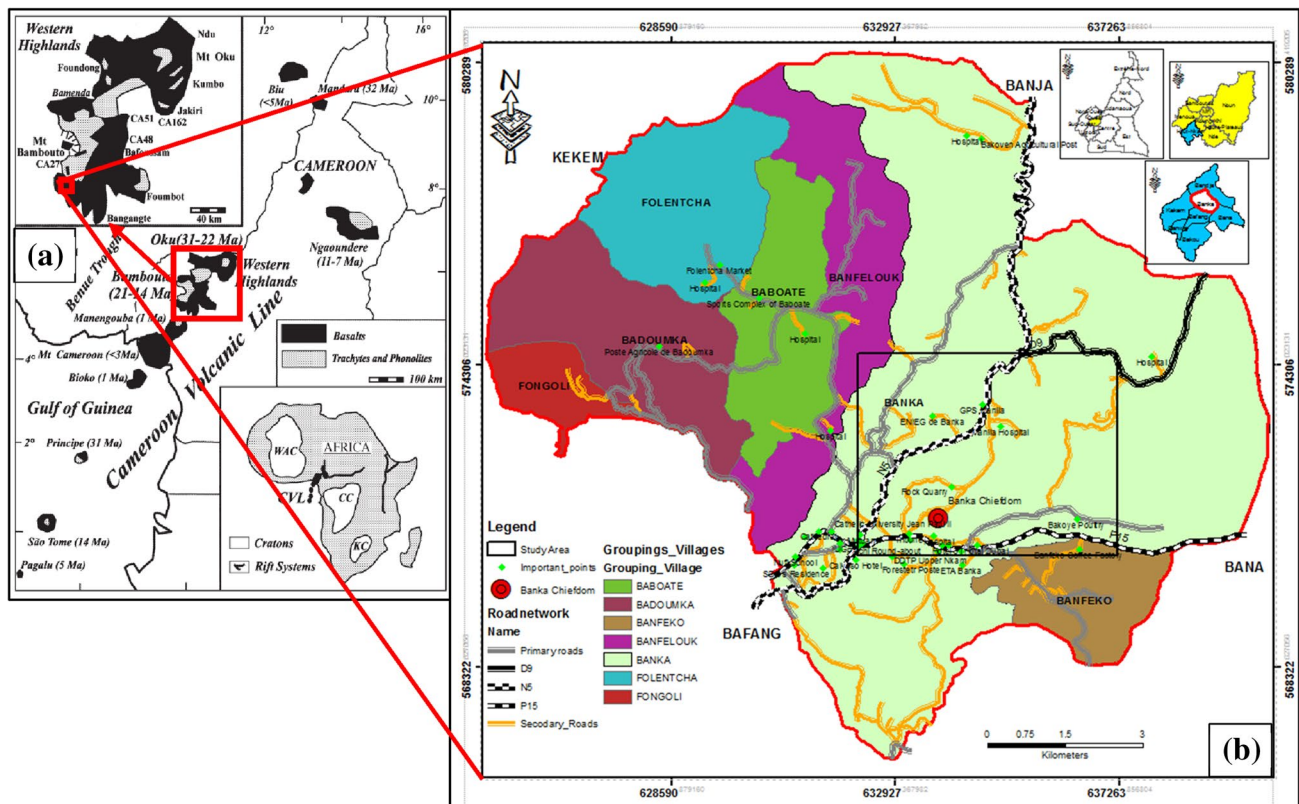


**Fig. 1** (a) Cameroon Volcanic line showing location of study area on Western highlands (top left inset), modified from [27]; (b) is the administrative location map. The black rectangle in the center refers to a 20km<sup>2</sup> zone of interest over whose SRTM DEM is shown

in (c) below. A detailed geologic mapping was done over (c) in order to obtain the geology thematic map (c) SRTM of of zone of interest within Banka subdivision



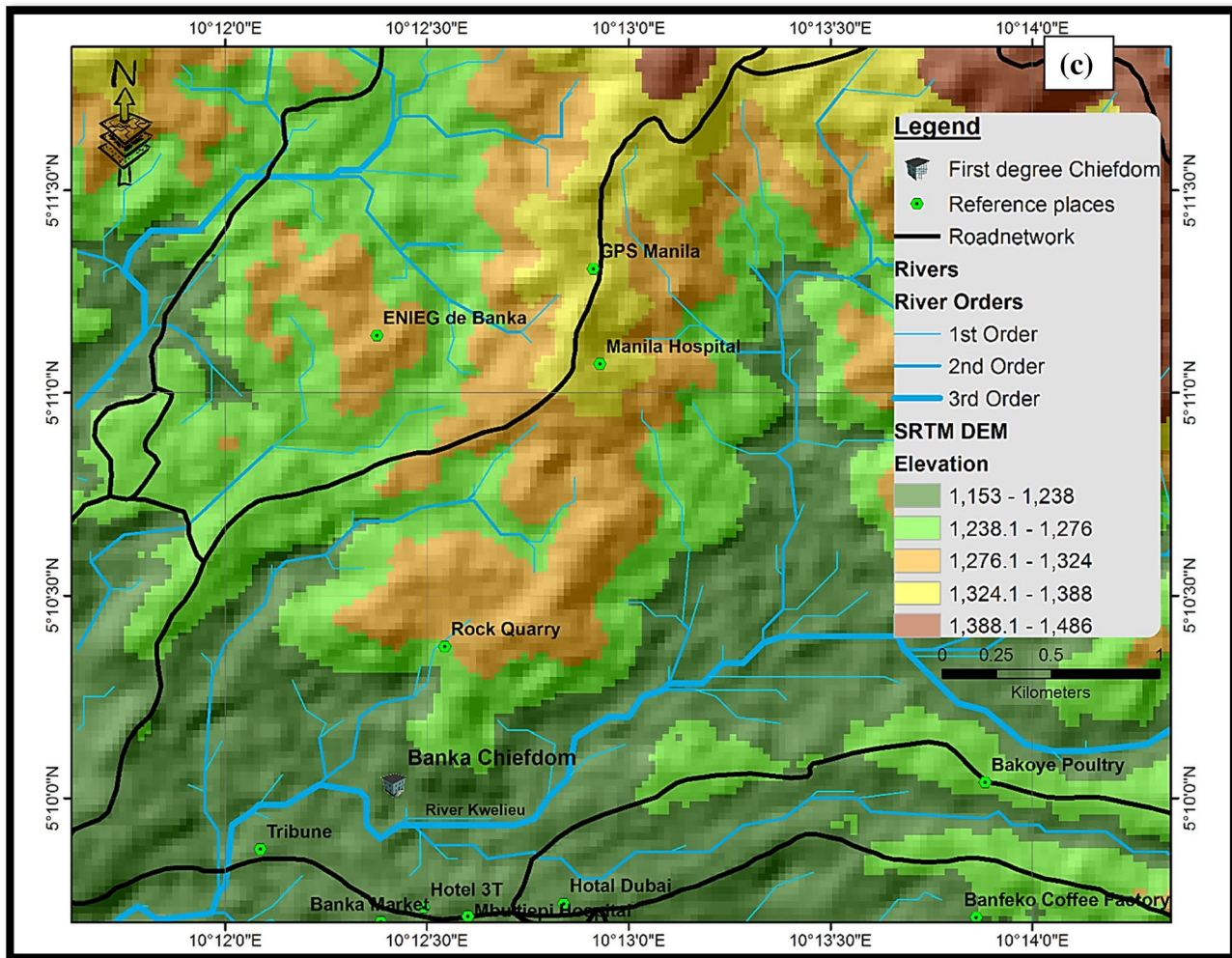


Fig. 1 (continued)

months of March and November with strong peaks in July and August. However increasing global warming-related droughts reduced this to barely between July and September. Temperatures also used to go up vertiginously only between December and February and fell sensibly between June and September, but these dry times time have now extended from November to June. Humidity is high with early morning ‘brunettes’ and twilight fog, especially during the dry season.

In terms of LULC, savannah shrub and herbaceous savanna separated with visible and fertile forest corridors dominate the vegetation. A varied range of dominant crops (coffee, cocoa, palm trees, market garden fruits and various food) can be observed in the area,

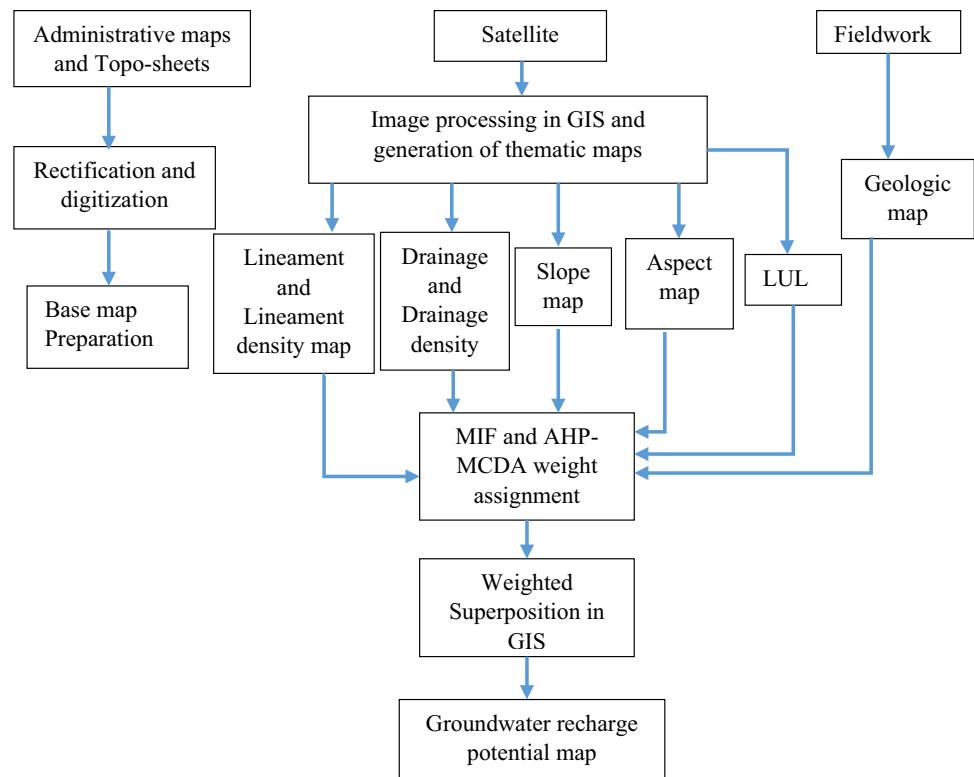
originating from the extensive subsistence agricultural lifestyle of the people. Though concentrated in the south of the study area, habitations flourish mostly along primary tarred (N5, D9) and secondary earth roads that serve the subdivision. Some households and bare land also spottily appear within the study area.

### 3 Material and methods

The methodology has been summarized in the workflow chart below (Fig. 2) and has been divided into the following activities;



**Fig. 2** Materials and methods used to delineate groundwater recharge potential zone



### 3.1 Preparation of thematic maps

Factors such as geology, slope, aspect, drainage density, lineament density and LULC were chosen to evaluate the  $GWR_{pot}$  based on data availability. Other factors like soil drainage and vertical permeability coefficient of the unsaturated zone may enhance the groundwater potential map, but unfortunately are not available for the area. Geologic mapping was carried out in the study area following a grid sampling methodology. A grid with grid cells  $400m \times 500m$  over  $20km^2$  was thrown over the area of interest and the rock samples at each grid node examined (in terms of their mineralogy (color and size), color, texture and structures like fractures and folds). These were registered in order to produce the geologic map layer of the area of interest. Apart from the geology layer, all the other factors were extracted from the SRTM-30m resolution and Landsat 8 of the study area obtained from the USGS database ([earthexplorer.usgs.gov](http://earthexplorer.usgs.gov)). In the GIS environment (ArcMap 10.2), grid cells of resolution  $16 \times 16m$  were used in order to ease calculations. The slope

and aspect were derived from the SRTM-extracted DEM following the methodology documented by [29] and analysis of errors and quality control of the derived dataset were done as described in [30] as well as [31] respectively. The drainage of the study area was also extracted from the DEM using the hydrology tool in ArcMap 10.2, and the drainage density was calculated and plotted using the line density tool. By using the Line module in PCI Geomatica v8 on the Landsat scene, the lineament map of the area was automatically extracted [32–34], from which the line density tool in ArcGIS 10.2 was again used to calculate and make the lineament density. The LULC was extracted from the Landsat 8 scene following a supervised classification with the Classification tool in ArcMap 10.2 ([https://appliedsciences.nasa.gov/week2\\_final](https://appliedsciences.nasa.gov/week2_final)). All these factors were prepared and saved as shapefiles compatible for integration within the GIS environment. The  $16 \times 16m$  grid maps for each factor were reclassified into five classes from 1 to 5, with the value of five attributed to categories that favor  $GWR_{pot}$  the most [2]. For example, the highest lineament density

**Fig. 3** Integrating factors using superposition principle of weighted overlay analysis to produce  $GWR_{pot}$  map of study area

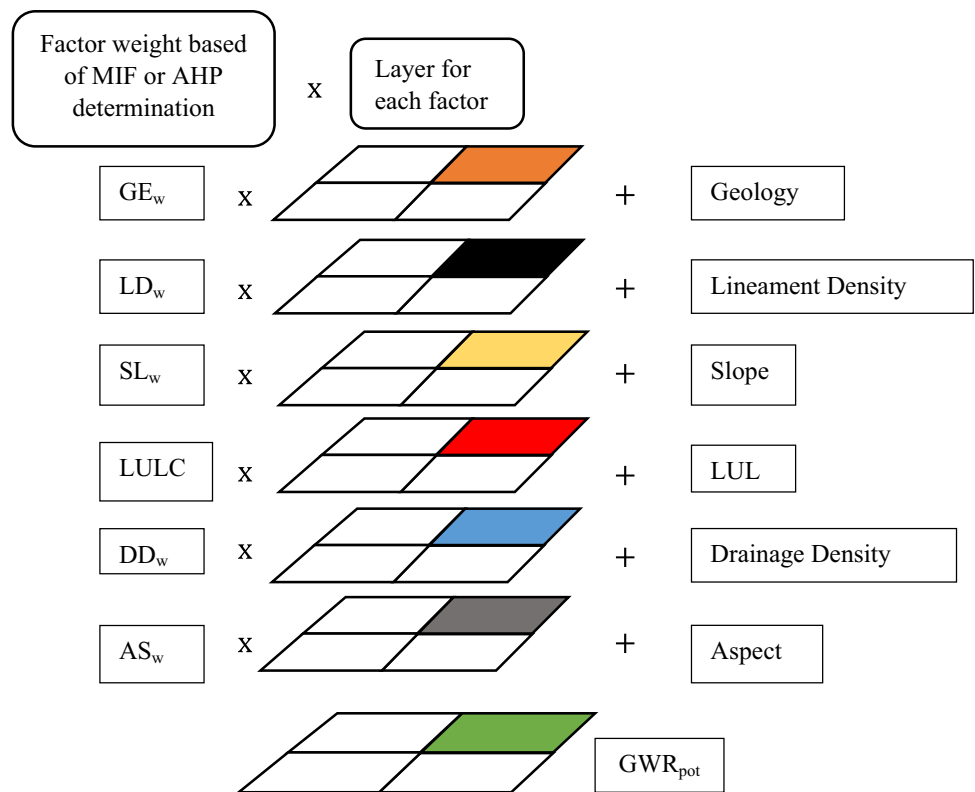
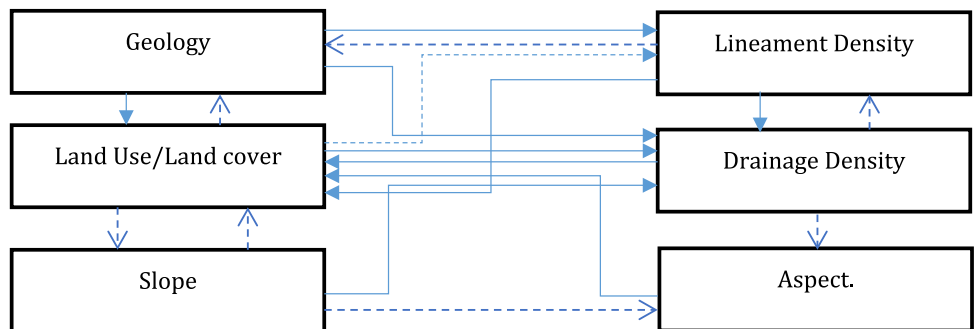


**Fig. 4** Suggested interrelationship between the multi influencing factors on the groundwater recharge potential zone



class was attributed 5 because these areas have the highest discontinuity and hence any precipitation or run-off will rather infiltrate.

$GWR_{pot}$  was finally calculated using the formula:

$$GWR_{pot} = (LD_r \times LD_w) + (DD_r \times DD_w) + (GE_r \times GE_w) + (SL_r \times SL_w) + (AS_r \times AS_w) + (LULC_r \times LULC_w) \quad (1)$$

where  $r$  &  $w$  are respectively the reclassified values and weight of the factors. This literarily means using the superposition principle to overlay the weightage ( $r \times w$ ) layers of

each factor on one another in a GIS environment (Fig. 3). Since the assigned weight per factor are subjective and may vary significantly in reality, we reduced uncertainty by using two different approaches to evaluate them including:

- The MIF approach, and
- The Analytical Hierarchy process of Multi-Criteria Decision analysis (AHP-MCDA)

**Table 1** Ratio or Random index values adopted from [36, 37]

n	1	2	3	4	5	6	7	8	9
RI	0.0	0.0	0.5	0.79	0.99	1.37	1.44	1.55	1.59

## 3.2 Assigning Weights

### 3.2.1 Multi-Influencing Factors (MIF) method

The MIF approach involves a sketch with the inter-relationship between the factors and assignment of weights according to the strength of the interrelationships [1, 2, 5, 22]. The sketch used for this study is shown in Fig. 4 and the continuous arrow lines represent major influences while the dash arrow represents minor influences. During weight assignment, continuous arrows from a factor are worth 1 while dash lines still going from a factor represent 0.5 [1, 2, 5], such that for every factor, its influence ( $w_f$ ) also called its weight will be the sum of the weights of all the lines that leave it. For example, a continuous line arrow points from DD to LULC and a dash line arrow from DD to Slope and LD. Therefore, the influence  $w_f$  of the factor DD on the other factors is 2 points (1 point + 0.5 + 0.5 points). Studies such as those of [1, 2, 5, 20] and [22] calculated the weight of their chosen factors in a similar manner. Since the final map of  $GWR_{pot}$  is a cumulative weightage, the relative weight  $w_{f,r}$  of each factor is determined following equation 2 below [2]:

$$W_{f,r} = \frac{w_f}{\sum_{i=1}^n w_f} \quad (2)$$

where  $w_f$  is the absolute value of the influence of the factor and  $n$  is the number of factors. The calculated weights (influence) and relative weight of each of the factors in this study.

### 3.2.2 Analytical Hierarchy Process of Multi-Criteria Decision Analysis (AHP-MCDA) method

Problems characterized by the influence of several parameters are best solved using Multi-Criteria Decision analysis (MCDA) [35]. AHP-based MCDA as described by [23] was also applied in this work to get the weight of the chosen factors from another angle. The pair-wise comparison matrix of the factors was obtained by assigning weights to each factor following the 1-9 scale suggested in [23, 35] where 1 = equal, 2 = weak, 3 = moderate, 4 = moderate plus, 5 = strong, 6 = strong plus, 7 = very strong, 8 = super strong, 9 = extreme importance. The Eigenvector technique was used to normalize the

**Table 2** Effect of influencing factors, relative rates and score for each potential factors

Factor	Major factor (A)	Minor factor (B)	Proposed $w_f$ (A+B)	Proposed MIF Weights ( $w_{f,r}$ ), %
LD	1+1	0.5	2.5	19.2
GE	1+1+1	0	3	23.1
DD	1	0.5+0.5	2	15.4
SL	1	0.5+0.5	2	15.4
AS	1	0	1	7.7
LULC	1	0.5+0.5+0.5	2.5	19.2
			$\Sigma=13$	$\Sigma=100$

assigned weights, after which the consistency test of the choice of weights between pairs was done using the consistency ratio that was calculated as follows:

$$CR = \frac{CI}{RI} \quad (3)$$

where CI is the consistency index and RI is the ratio or random index.

$$CI = \frac{\lambda_{max} - n}{n - 1} \quad (4)$$

In CI,  $n$  = number of factors and  $\lambda$  = average value of consistency vector (max eigen value). RI is a value that depends on 'n' values as seen in Table 1.

## 4 Results and Discussions

### 4.1 Weightage calculations

Two methods were used to assign weights to the factors chosen to delineate the  $GWR_{pot}$  in this study. The multi-influencing factors (MIF) of  $GWR_{pot}$  zones namely LD, GE, LULC, SL, DD and AS were assigned corresponding weights (Table 1), after thorough examination using the chart in Fig. 4. The factors are interdependent, each having either a major or minor influence on the other and hence helping to delineate the  $GWR_{pot}$  zones. From the MIF methodology of weight assignment, the GE, LD and LULC are the most influential factors. Studies like those of [1, 2, 5, 18] and [38], which used MIF also reached similar conclusions.



**Table 3** Normalize pair-wise matrix showing normalized AHP weights ( $W_i$ ) in %. Consistency ratio was less than 0.1 (precisely 0.0809) with RI value of 1.37 (i.e.  $n = 6$  in Table 3 above)

Factor	LD	GE	SL	LULC	DD	AS	Sum	Normalized weight ( $W_i$ )	$W_i$ , %
LD	0.167286	0.144654	0.183844	0.178116	0.247154	0.192047	1.1131	0.185517	18.55
GE	0.171004	0.289308	0.175487	0.323847	0.205961	0.160039	1.325646	0.220941	22.09
SL	0.163569	0.192872	0.250696	0.161923	0.102981	0.174588	1.046629	0.174438	17.44
LULC	0.178439	0.192872	0.167131	0.107949	0.196154	0.174588	1.017132	0.169522	16.95
DD	0.171004	0.096436	0.083565	0.080962	0.068654	0.128031	0.628652	0.104775	10.48
AS	0.148699	0.083857	0.139276	0.147203	0.179097	0.170708	0.86884	0.144807	14.48

**Table 4** Reclassified values of the value ranges of each factor. The overall MIF weight is obtained from the product of factor class reclassified value and factor MIF weight. The overall AHP weight is obtained from the product of factor class reclassified value and factor AHP weight.

Factors	Value range	Reclassified value	Contribution to GWRpot	Overall MIF Weight, %	Overall AHP Weights, %	Ave. overall Weight, %
Lineament density, LD, (km/km <sup>2</sup> )	< 2	1	Very low	19.2	18.55	18.88
	2 - 4	2	Low	38.4	37.1	37.75
	4 - 6	3	Medium	57.6	55.65	56.63
	6 - 8	4	High	76.8	74.2	75.50
	> 8	5	Very high	96	92.75	94.38
Drainage density, DD, (km/km <sup>2</sup> )	> 15	1	Very low	15.4	10.48	12.94
	11- 15	2	Low	30.8	20.96	25.88
	7 - 11	3	Medium	46.2	31.44	38.82
	3 - 7	4	High	61.6	41.92	51.76
	< 3	5	Very high	77	52.4	64.70
Geology, GE	Normal Gneisses	1	Very low	23.1	22.09	22.60
	Granites	2	Low	46.2	44.18	45.19
	Augen Gneisses	3	Medium	69.3	66.27	67.79
	Pegmatites	4	High	92.4	88.36	90.38
	Basalts	5	Very high	115.5	110.45	112.98
Slope, SL, (°)	> 28	1	Very low	15.4	17.44	16.42
	18 – 28	2	Low	30.8	34.88	32.84
	12 – 18	3	Medium	46.2	52.32	49.26
	6 – 12	4	High	61.6	69.76	65.68
	< 6	5	Very high	77	87.2	82.10
Aspect, AS	Flat terrain, South	1	Very low	7.7	14.48	11.09
	Southeast Southwest	2	Low	15.4	28.96	22.18
	East, west	3	Medium	23.1	43.44	33.27
	Northeast Northwest	4	High	30.8	57.92	44.36
	North	5	Very high	38.5	72.4	55.45
Land Use and Land Cover, LU	Urban area	1	Very low	19.2	16.95	18.08
	Forest	2	Low	38.4	33.9	36.15
	Water	3	Medium	57.6	50.85	54.23
	Bare land	4	High	76.8	67.8	72.30
	Agriculture	5	Very high	96	84.75	90.38

Weight assignation using the AHP-MCDA method produced weightages more or less similar to those of MIF after normalization as seen in Table 2. Since

these produce a consistency index < 0.1, they are acceptable and usable in MCDA. From the weightages obtained using AHP, GE, LD and SL are the most

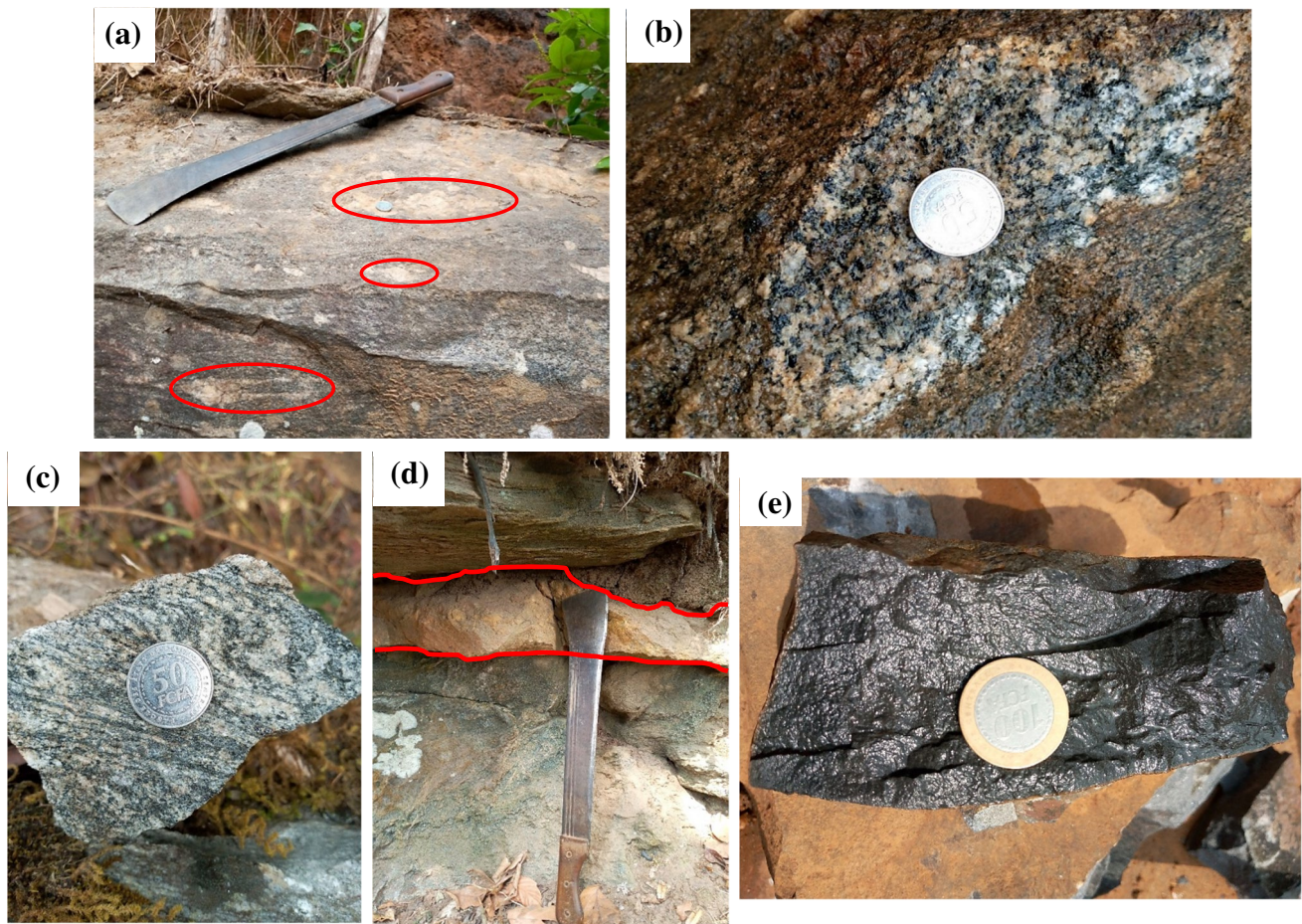


**Fig. 5** **a** Sub outcrop of Augen gneiss. Ellipses on plate shows Auga. **b** Granite samples making up the study area. **c** Gneiss showing millimetric folds. **d** Ten (10) cm thick pegmatite intruding in a gneiss. **e** Basalt

prominent factors affecting  $GWR_{pot}$  in the area. LULC comes almost indistinguishably after SL, also making SL a factor of major influence as it is expected to be. Similar weightages from AHP and classification of importance have also been obtained by [39] and [40].

Finally, by multiplying each factor class reclassified value in Table 4 by the corresponding class MIF or AHP weight, the overall weights of the factors from either MIF or AHP (Table 4) were obtained. An average overall weight that is obtained by averaging the overall MIF and AHP weights is also shown in Table 4. These overall weights were then integrated into their thematic map classes ArcGIS 10.2 and cumulated per map cell using the Union tool to finally produce the  $GWR_{pot}$  map that delineates the various potential recharge zones.

## 4.2 Geologic map

A geological mapping campaign following a grid of 400x500m was carried out in the study area, in a bid to update the geological information of the area and to ground truth the remotely sensed data. A geologic map of the study area at a scale of 1:15,000 was produced and shows that the area hosts five main rock types; granites, gneisses, pegmatites and basalt (Fig. 5a–e). Basalts dominate the study area, followed by the gneisses. Granites and pegmatites outcrop mainly in the north of the study area. These hardrocks are impervious and will host and transmit water based on their degree of fracturing which is related to their tensile strength or ability to resist brittle deformation. According to the studies of [41–43], petrological parameters such as grain size and grade

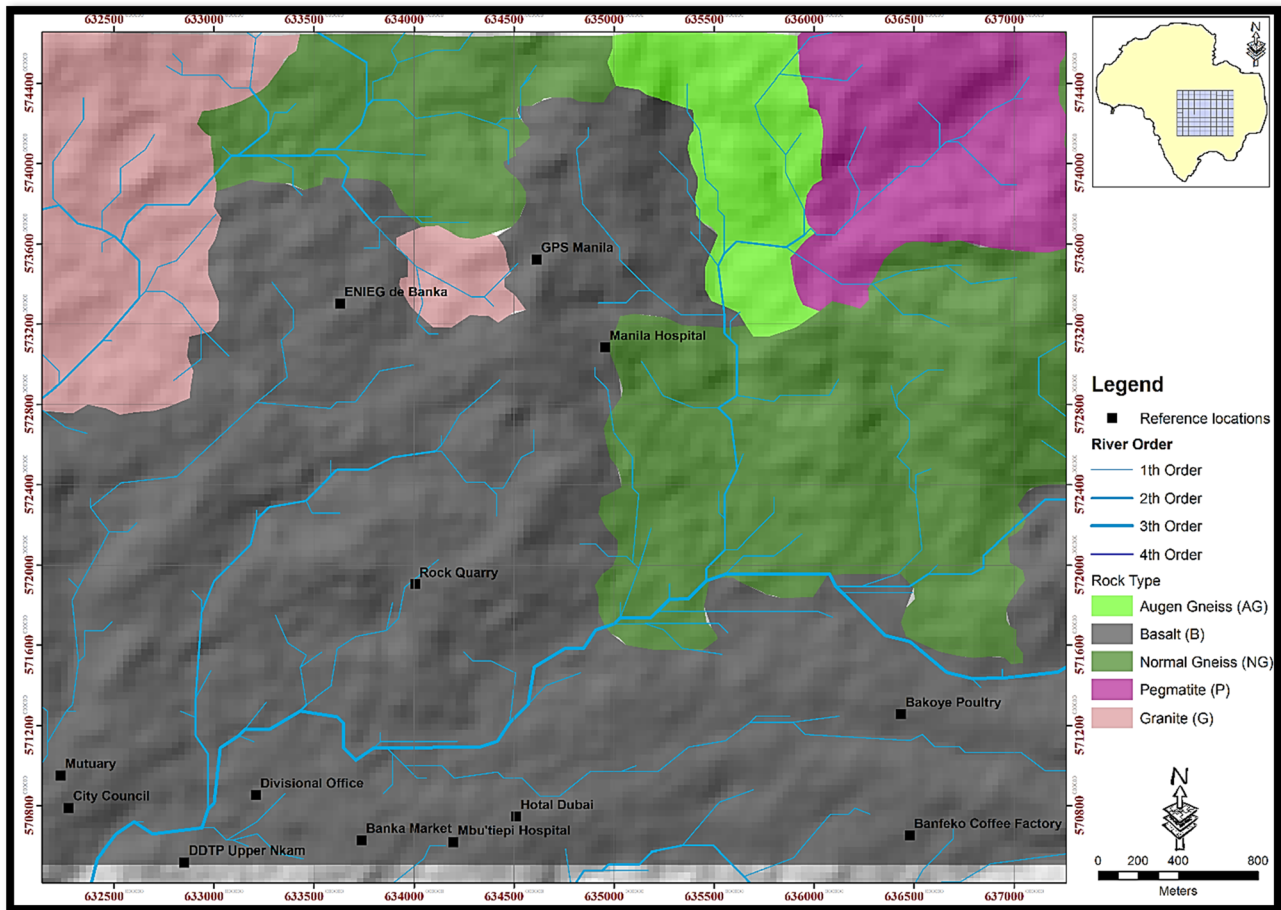


**Fig. 6** Geologic map of study area

of metamorphism play a dominant role in fracture formation, there by being indirectly related to groundwater occurrence. Based on these parameters, the fracture tendency of the rocks in the study area should increase from normal gneisses, through granites, augen gneisses, pegmatites and finally basalts. These are corroborated by presence of more lineament in basalts than in normal gneisses (Fig. 6). Several structures ranging from millimetric folds and veins through quartz and pegmatite filled veins and metric fractures were identified in the rocks. These show that the area has suffered intense structural deformation that can be associated to the volcanic activities of the CVL [43–50].

### 4.3 Lineament density Map

Structurally controlled linear or curvy linear features identified in satellite imagery as linear alignments are called lineaments [1, 2]. Underlying structures usually manifest on surface topography through these features. The fact that they usually form due to faulting and fracturing generally associates them to secondary porosity and permeability that permits storage and flow of groundwater both vertically and horizontally [1]. Therefore, the density of lineaments in an area can be translated in groundwater recharge and groundwater potential. After the automatic extraction of the lineaments from the Landsat image of the study area, the LD map (Fig. 7) was developed using the line density tool in ArcGIS 10.2. The medium, high and very high



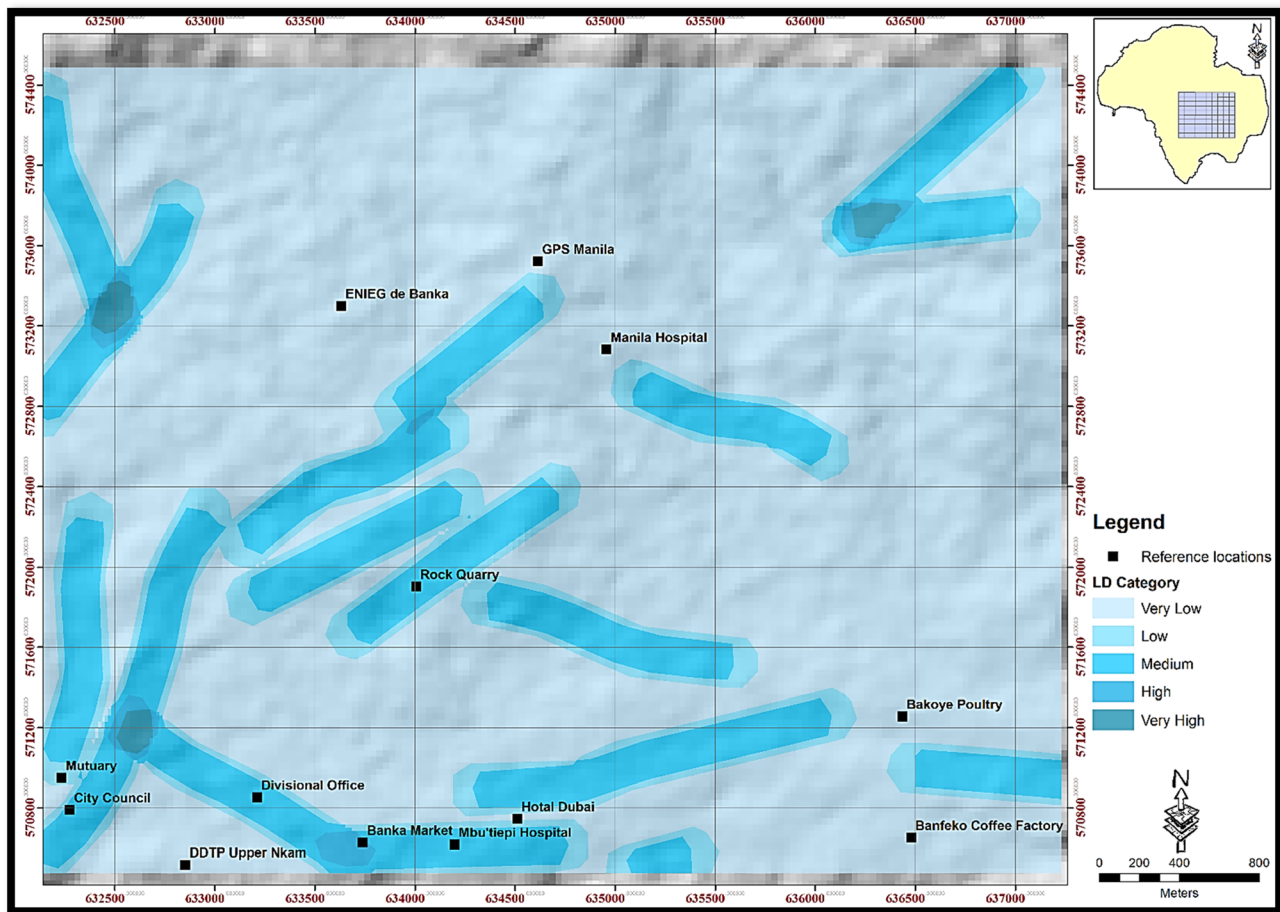


**Fig. 7** Lineament density map of study area. Medium, high and very high densities mainly appear in the central, south and western parts of study area

lineament densities (all above  $4\text{km}/\text{km}^2$ ) are those of high interest, as they will ease water percolation into the underground reservoirs. These classes of interest are mostly seen in the central, southern and western sectors of the study area.

#### 4.4 Land Use and Land Cover (LULC)

The LULC presents forest (40.82%), agricultural (28.10%) and bare land (8.20%) land patterns that favor seepage and cover almost all the study area. The Urban area (18.70%) and waterbodies (4.18%) land patterns allow very little percolation. These LULC classes (Fig. 8) were delineated from Landsat 8 through a supervised classification in ArcGIS 10.2 and intense verification in the field. Similar methodologies were used to produce the LULC that were used in the evaluation of  $\text{GWR}_{\text{pot}}$  [20, 21, 51 and 52,] and of artificial recharge zones [18].

#### 4.5 Slope

Slope is a very important factor in groundwater studies. It has been used in numerous studies to evaluate infiltration, potential location of groundwater and location of artificial recharge zones [1, 2, 7, 10, 11, 12, 13, 14, 15, 18, 20 and 21]. Rapid run-off usually results from high-angle slopes, hence permitting little water infiltration during and after precipitation [1, 53, and 54]. By analogy, low angle slopes are those of interest for groundwater recharge. Processing of the SRTM-30m data of the study area using the spatial analyst tool in ArcGIS 10.2 produced the slope map (Fig. 9) that has five main classes. The  $0\text{-}6^\circ$  slopes fall are the "Very good" class as these areas are flat to nearly flat, allowing for higher infiltration times. Slightly steeper topography with slopes between  $6\text{-}12^\circ$  are considered "Good" for groundwater recharge as they produce some run-off and offer lesser infiltration time. Areas with slope between  $12\text{-}18.5^\circ$  and those with slopes

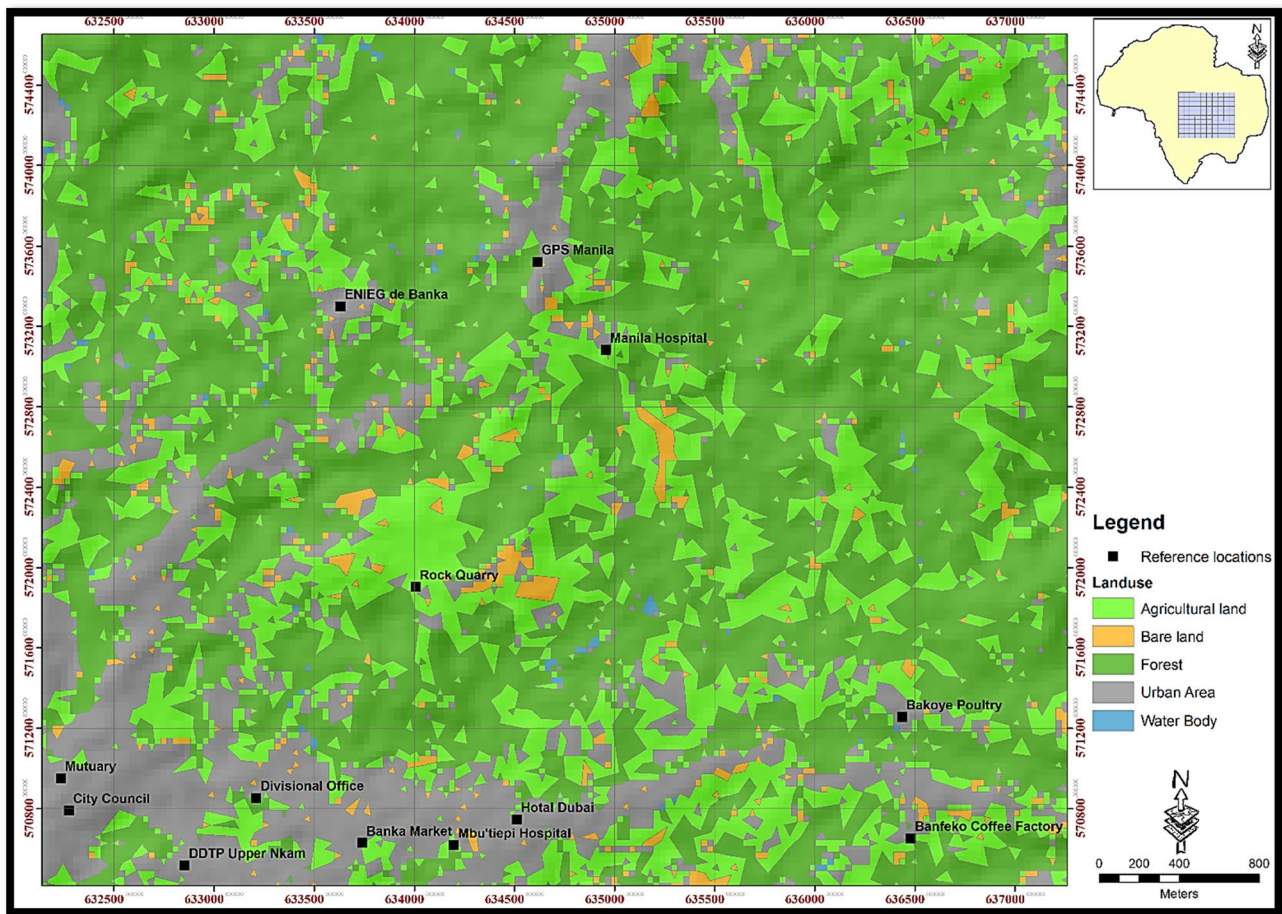


**Fig. 8** Land Use and Land Cover map of study area (LULC). It clear from this that the forest and agricultural land covers are the most predominant, followed by built land. Though present the water bodies in the study area are not very large, and there is very little bare land

between 18.5–28° fall in the “Moderate” and “Poor” classes respectively since they produce much run-off. Finally, all zones with slopes >28° fall in the “Very poor” class. [1] proposed a similar classification.

#### 4.6 Drainage density

The measure of the total length of the streams of all orders in a unit area is called drainage density and it defines the closeness of stream channels in an area. It inversely relates to the permeability of an area since the lower the permeability of an area the lower the infiltration of precipitation and therefore the higher the concentration of run-off that can be seen in part as streams. Drainage

density is commonly used in groundwater studies [1, 2, 4, 13, 22, 35, 38, 55]. The drainage density map (Fig. 10) of the study area was developed using the line density tool in ArcGIS 10.2 on the drainage map that was extracted from the SRTM-30m satellite image using the Hydrology tool in the same ArcGIS. Five classes are identified on this map including “Very low” (0–3km/km<sup>2</sup>), “Low” (3–5km/km<sup>2</sup>), “Medium” (6–10km/km<sup>2</sup>), “High” (11–15km/km<sup>2</sup>) and “Very high” (> 15km/km<sup>2</sup>). The very low, low and medium drainage density are those that are of interest as their inverse relationship earlier mentioned imply higher permeabilities and hence more surface water infiltration to recharge the underground reservoirs. These are seen in the map



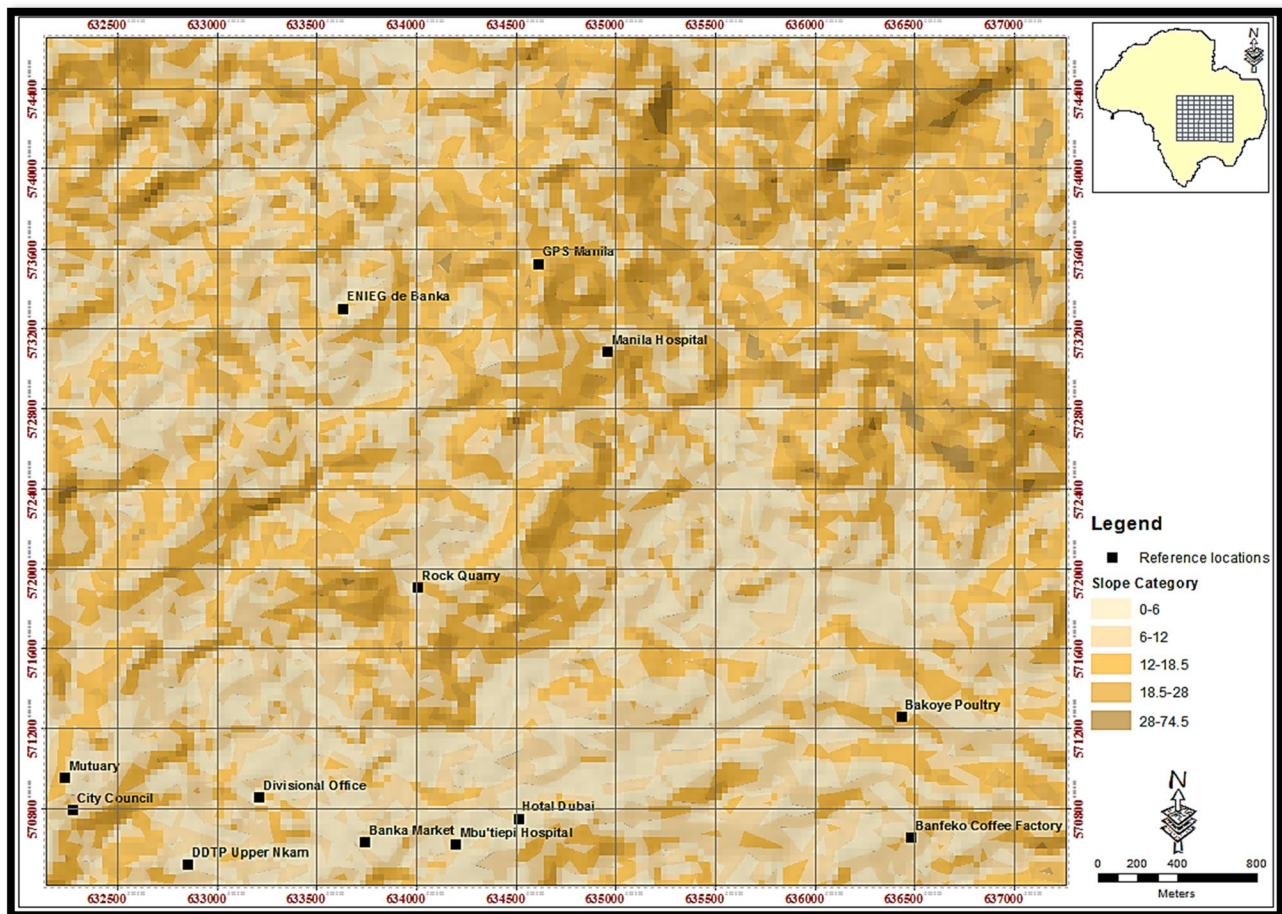


Fig. 9 Slope map of study area

as corridors that runs NE-SW across the center of the map, N-S in the eastern portion of the map and almost E-W in the southern portion.

#### 4.7 Aspect

Aspect is defined as the compass direction that a topographic slope faces, and is used here as in [2] to qualitatively give a measure of the amount of solar radiation the surfaces in the study area receive. This measure can be in turn used to estimate the amount of evapotranspiration, which is inversely proportion to groundwater recharge since high evapotranspiration means high water uptake by plants to replace the lost one due to the Sun's heat and vice versa. The aspect map (Fig. 11) of the study area was developed

using the aspect tool of ArcGIS 10.2. Since we are in the tropics, cloud cover is thinnest and is assumed a relatively constant factor. Flat facing slopes are expected to receive the highest amount of radiation, given that the sun heats them all day long and is hottest and overhead around noon. This implies they will have a high value of evapotranspiration and hence were put in the "Very low" class meaning they will have lowest groundwater recharge potential. Following a similar logic, the SE & SW fall in the "Low" class, the E & W in the "Moderate" class, the NW & NE in the "High" class and the N, into the "Very high" class. Aspects in the "High and "Very high" classes (which are of interest) appear as almost E-W and NE-SW trending non continuous adjacent corridors in the S, W, NW, NE and E portions of the study



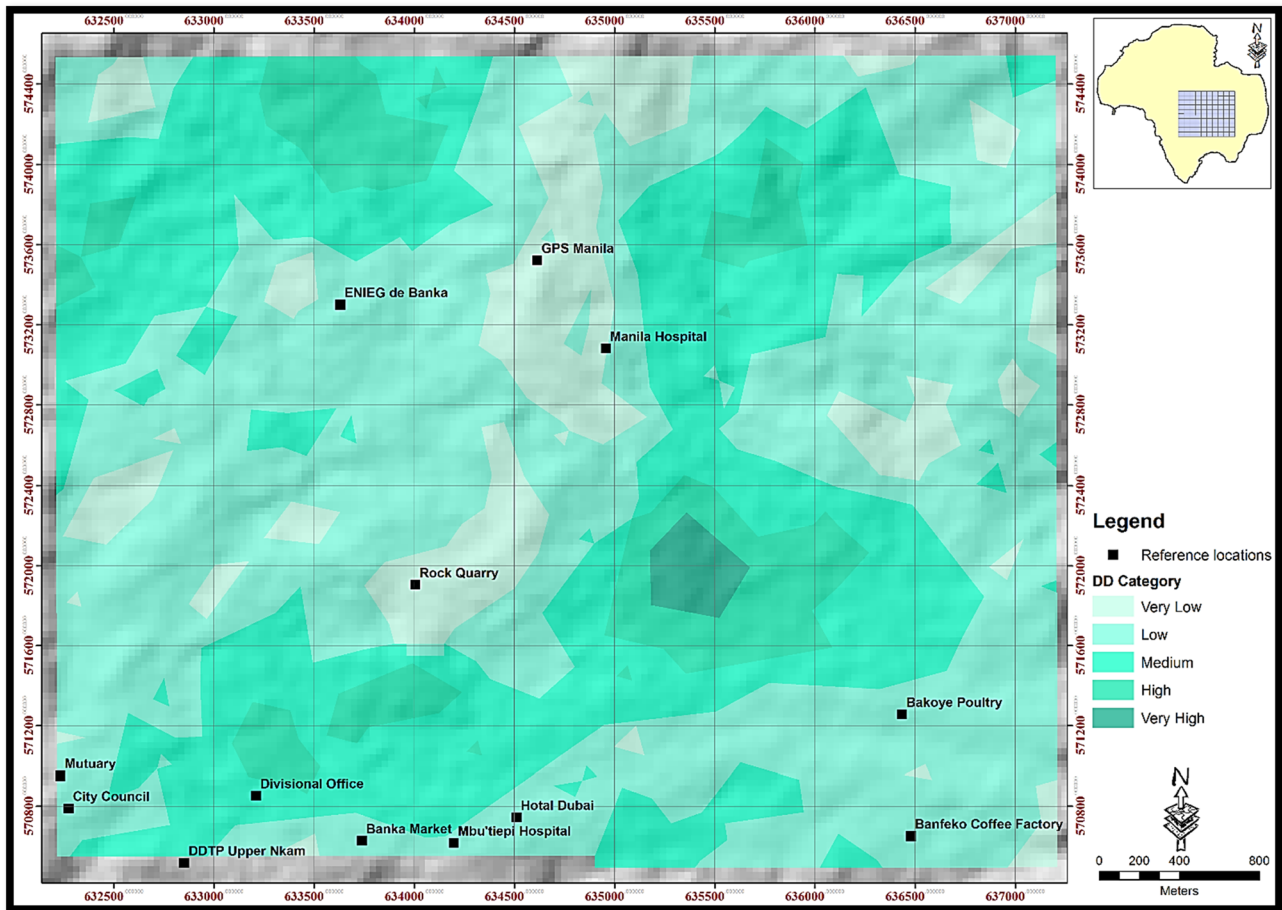


Fig. 10 Drainage density map of study area

area. These zones coincide with most of the parts of the study area where the lineament densities are high and the Drainage Density values are low.

#### 4.8 Groundwater recharge potential map

The groundwater recharge potential of the study area was produced by integration using weighted overlay in a GIS environment of various thematic maps: GE, LD, DD, SL, LULC and AS. Once the overall MIF and AHP weights and the Average overall weights were added to the different thematic maps, the maps were overlaid on one another using the Union tool in ArcGIS. The cumulative weight (CW) of each resulting cell, which is the sum of the weights of the same cell in the layer of each thematic map, was then calculated and used to describe the GWR<sub>pot</sub>. Hence, the GWR<sub>pot</sub> zones were delineated

by grouping integrated map cells into classes based on their CW. This led to the delineation of five GWR<sub>pot</sub> classes: the “Very low” with CW in the interval 16-211.73, “Low” with CW in the interval 211.73-268.45, “Moderate” with CW in the interval 268.45- 318.68, “High” with CW in the interval 318.68-388.25 and the “Very high” class with weights in the interval 388.25-487.05. The GWR<sub>pot</sub> map (Fig. 12) shows that about 60% of the study area has a “Moderate” to “Very high” recharge potential, distributed in the south, west-northwest and the north-northeast of the map, implying that any drop of precipitation that falls in these areas have a greater chance of infiltrating and hence recharging the groundwater reservoirs. This map can be validated by the fact that perineal flowing boreholes and wells in the study area all fall with the zones marked to have moderate, high or very high recharge potential. [1] and [2] used similar arguments

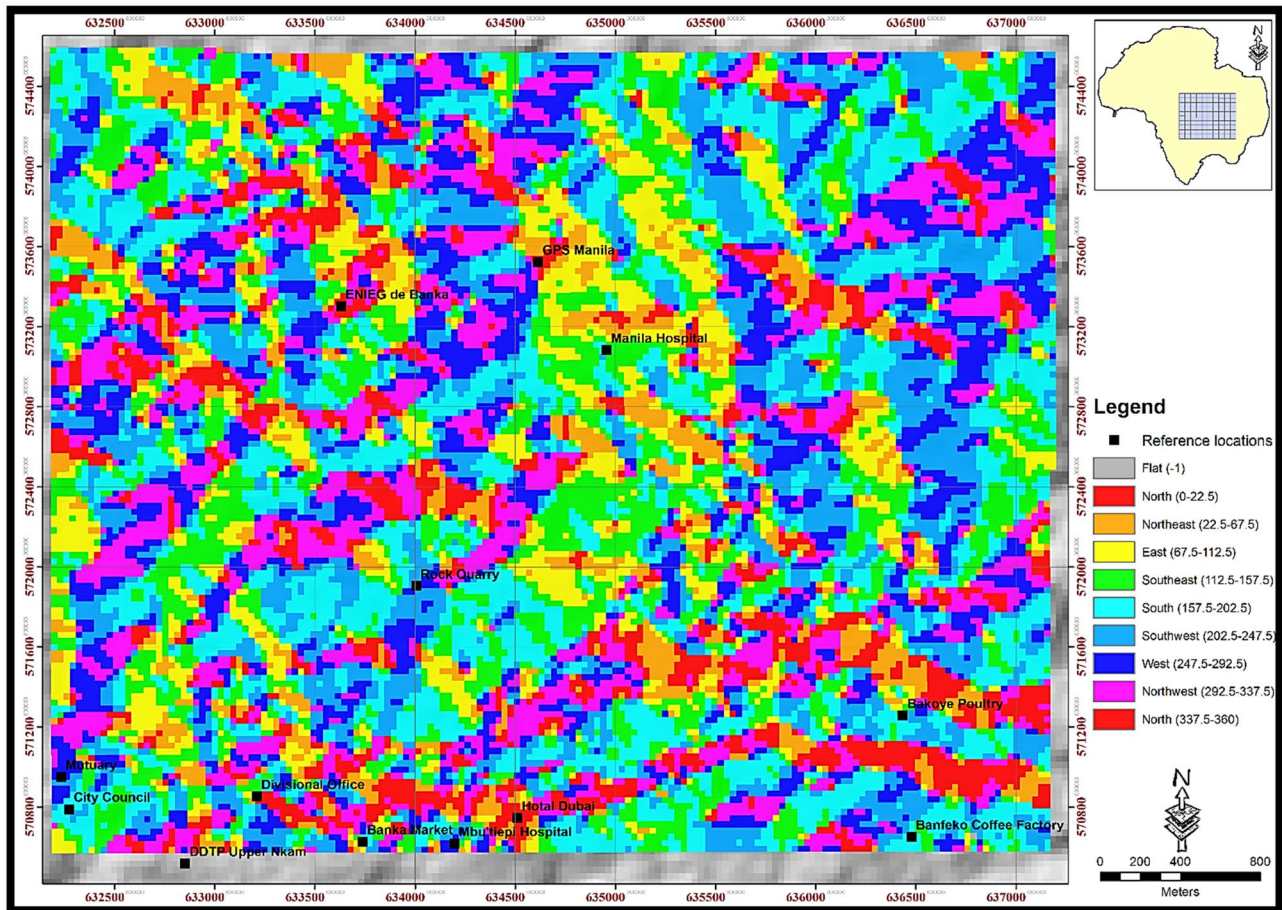


Fig. 11 Aspect map of study area

when validating their groundwater potential and potential groundwater recharge zone models, hence implying our proposed model is accurate.

## 5 Conclusions

Groundwater is the safest source of water and forms only from the infiltration of surface water to recharge underground reservoirs. This means the amount and location of groundwater will greatly be enhanced if we know the recharge zones, especially in hardrock terrains that have very low primary porosity and permeability. However, evaluation of potential recharge zones by conventional methods is generally costly and time consuming at large geographic coverage. Since several studies show that GIS and remote sensing techniques offer less costly and faster means of evaluating recharge, we used them to delineate the  $GWR_{pot}$  zones in the Banka subdivision of Cameroon, located within the hardrock of the CVL. A number of rock-informative layers of factors

that are relevant to groundwater recharge including LULC, DD, LD, SL, GE and AS were outlined and superposed on each other. To reduce the uncertainty of the final weights of each factor the Multi-Influencing Factor (MIF) and Analytical Hierarchy Process of Multi-Criteria Decision Analysis (AHP-MCDA) were used to evaluate the relative importance (weight) of each factor. The average weights for each factor was to produce the weighted layers which were finally integrated in the GIS environment. Five descriptive classes namely: "Very low", "Low", "Moderate", "High", and "Very high" were delineated on the final  $GWR_{pot}$  map. Our results show that urbanized areas and the hills with steep slopes and high drainage densities made of unfractured gneisses and granitic rocks have poor recharge potentials. Meanwhile, lowland and gently-sloping hills made up of fractured rocks, lower drainage densities and agricultural or bare land have the highest groundwater recharge potential. The fact that 60% of the study area has "moderate" to "Very high" recharge potential implies the study area could host groundwater and hence this  $GWR_{pot}$  map can be



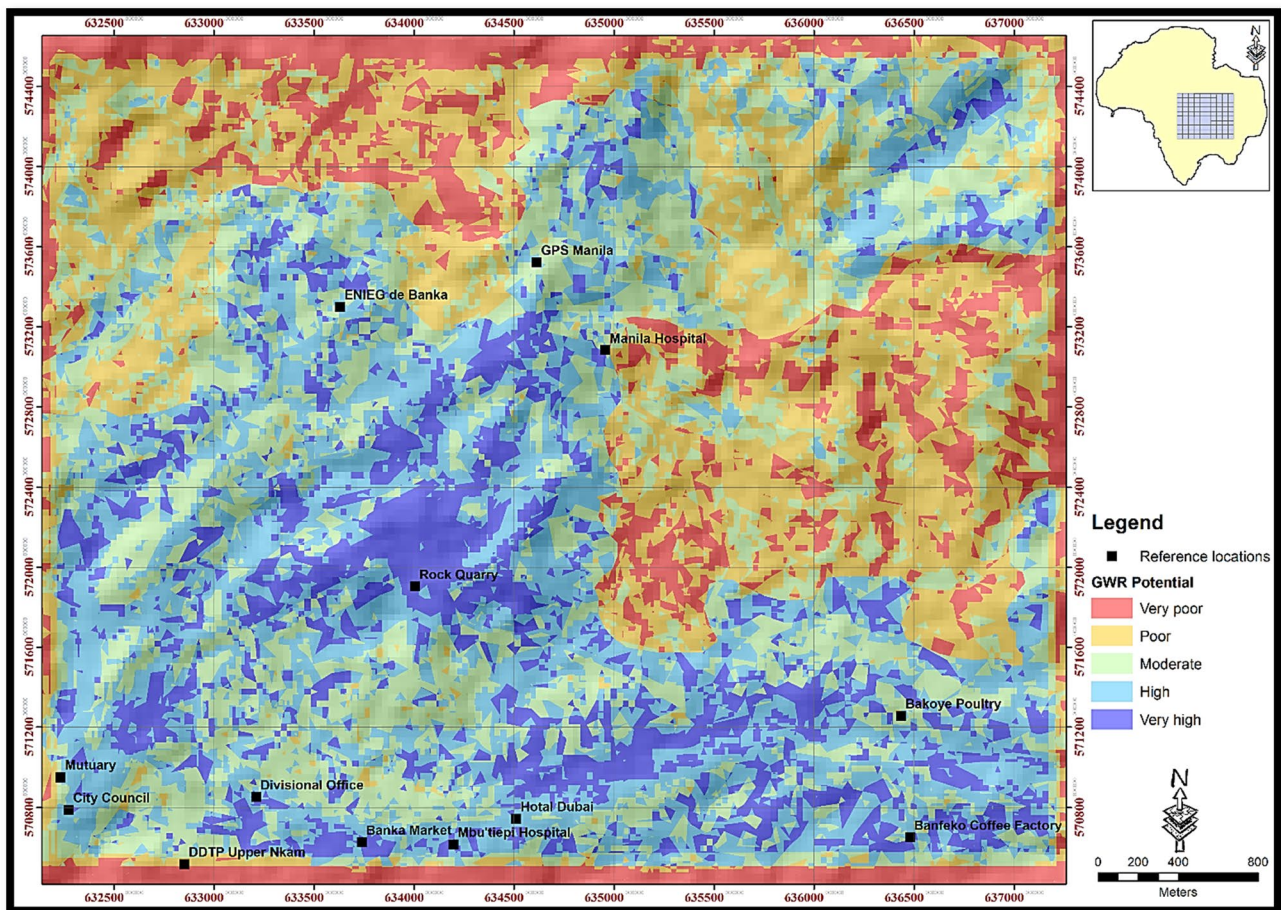


**Fig. 12** Groundwater recharge potential map of study area

used as an initial guide for groundwater exploration in the area. Perspectives involve applying this study over the subdivision and even the Region as a whole in order to produce regional (small-scale) maps that give detail distribution of recharge zones, hence better planning groundwater exploration programs. The unavailability of vertical and horizontal soil permeability data is a drawback to our  $GWR_{pot}$  map and hence we recommend that the subsequent studies obtain and integrate this factor for a more accurate model.

**Acknowledgments** Our deepest thanks to Mr. Kuisseu Thierry Stephane and Mr. Jules Ngantouo for their enriching physical and technical inputs during the geological mapping stage of the project.

**Authors' contributions** Mbohlieu Tchawe YOSSA, Anatole E. DJIETO LONDON, and Christopher M. AGYINGI did the conception and design of. Material preparation, data collection and analysis were performed by Mbohlieu Tchawe YOSSA, Junior AGBOR-TAKU, Yves N. SHANDINI, Crayton Enga BESSONG. The first draft of the manuscript was written by Mbohlieu Tchawe YOSSA and restructured for better reader experience and understanding by Junior AGBOR-TAKU. All authors

commented on previous versions of the manuscript and have read & approved the final manuscript.

**Funding** The authors declare that no funds, grants, scholarship or other supports were received during this research.

**Data availability** The Landsat 8 and SRTM data are available at [earth-explorer.usgs.gov](http://earth-explorer.usgs.gov). The geologic data and shapefiles of the study area can be obtained on demand from the corresponding author.

## Declarations

**Conflict of interest** The authors have no relevant financial or non-financial interests to disclose.

**Open Access** This article is licensed under a Creative Commons Attribution 4.0 International License, which permits use, sharing, adaptation, distribution and reproduction in any medium or format, as long as you give appropriate credit to the original author(s) and the source, provide a link to the Creative Commons licence, and indicate if changes were made. The images or other third party material in this article are included in the article's Creative Commons licence, unless indicated otherwise in a credit line to the material. If material is not



included in the article's Creative Commons licence and your intended use is not permitted by statutory regulation or exceeds the permitted use, you will need to obtain permission directly from the copyright holder. To view a copy of this licence, visit <http://creativecommons.org/licenses/by/4.0/>.

## References

1. Magesh NS, Chandrasekar N, Soundranayagam JP (2012) Delineation of groundwater potential zones in Theni district, Tamil Nadu, using remote sensing. *GIS MIF Tech. Geosci Front* 3(2):189–196
2. Singh SK, Zeddies M, Shankar U, Griffiths GA (2018) (2018) Potential groundwater recharge zones within New Zealand. *Geosci Front*. <https://doi.org/10.1016/j.gsf.2018.05.018>
3. Maqsoom A, Aslam B, Khalid N, Ullah F, Anysz H, Almaliki AH, Almaliki, AA, Hussein EE (2022) Delineating groundwater recharge potential through remote sensing and geographical information systems. *Water* 14, 1824
4. Freeze RA, Cherry JA (1979) GIS based surface hydrological modelling in identification of groundwater recharge zones. *Int J Remote Sens* 25:e5759–e5770
5. Yeh HF, Cheng YS, Lin HI, Lee CH (2016) Mapping groundwater recharge potential zone using a GIS approach in Hualian River Taiwan. *Sustai Environ Res* 26 (1), 33e43.
6. Jaiswal R, Mukherjee S, Krishnamurthy J, Saxena R (2003) Role of remote sensing and GIS techniques for generation of groundwater prospect zones towards rural development approach. *Int J Remote Sens* 24(5):993–1008
7. Thapa R, Gupta S, Guin S, Kaur H (2017) Assessment of groundwater potential zones using multi-influencing factor (MIF) and GIS: a case study from Birbhum district, West Bengal. *Appl Water Sci* 7(7):e4117–e4131.
8. Thorpe HR, Scott DM (1999) An evaluation of four soil moisture models for estimating natural ground water recharge. *J Hydrol (New Zealand)* 38(2):179–209
9. White PA, Hong YS, Murray DL, Scott DM, Thorpe HR (2003) Evaluation of regional models of rainfall recharge to groundwater by comparison with lysimeter measurements, Canterbury New Zealand. *J Hydrol (New Zealand)* 42(1):39–64
10. Saraf AK, Choudhury PR (1998) Integrated remote sensing and GIS for groundwater exploration and identification of artificial recharge sites. *Int J Remote Sens* 19:1825–1841.
11. Solomon S, Quiel F (2006) Groundwater study using remote sensing and geographic information systems (GIS) in the central highlands of Eritrea. *Hydrogeol J* 14(5):729–741
12. Chenini I, Mammou AB, El May M (2010) Groundwater recharge zone mapping using GIS-based multi-criteria analysis: a case study in Central Tunisia (Maknassy Basin). *Water Res Manag* 24(5):921–939
13. Hammouri N, El-Naqa A, Barakat M (2012) An integrated approach to groundwater exploration using remote sensing and geographic information system. *J Water Res Protect* 4:e717–e724. <https://doi.org/10.4236/jwarp.2012.49081>
14. Kaliraj S, Chandrasekar N, Magesh N (2014) Identification of potential groundwater recharge zones in Vaigai upper basin, Tamil Nadu, using GIS-based analytical hierarchical process (AHP) technique. *Arab J Geosci* 7 (4), 1385e1401.
15. Patil SG, Mohite NM (2014) Identification of groundwater recharge potential zones for a watershed using remote sensing and GIS. *Int J Geomat Geosci* 4(3):485
16. Mseli Zaina Hussein, Mwegoha William John, Gaduputi Sankaranna (2021) Identification of potential groundwater recharge zones at Makutupora basin. Dodoma Tanzania, Geol, Ecol Landsc., <https://doi.org/10.1080/24749508.2021.1952763>
17. Sener E, Davraz A, Ozcelik M (2005) An integration of GIS and remote sensing in groundwater investigations: a case study in Burdur, Turkey. *Hydrogeol J* 13:826–834
18. Senanayake I, Dissanayake D, Mayadunna B, Weerasekera W (2016) An approach to delineate groundwater recharge potential sites in Ambalantota, Sri Lanka using GIS techniques. *Geosci Front* 7(1):115–124
19. Krishnamurthy J, Venkatesa Kumar N, Jayaraman V, Manivel M (1996) An approach to demarcate ground water potential zones through remote sensing and a geographical information system. *Int J Remote Sens* 17(10):1867–1884
20. Shaban A, Khawlie M, Abdallah C (2006) Use of remote sensing and GIS to determine recharge potential zone: the case of Occidental Lebanon. *Hydrogeol Journal* 14:433–443
21. Prasad RK, Mondal NC, Banerjee P, Nandakumar MV, Singh VS (2008) Deciphering potential groundwater zone in hard rock through the application of GIS. *Environ Geol* 55:467–475
22. Yeh HF, Lee CH, Hsu KC, Chang PH (2009) GIS for the assessment of the groundwater recharge potential zone. *Environ Geol* 58(1):185–195
23. Saaty TL (1980) *The Analytic Hierarchy Process; Planning, Priority Setting, Resource Allocation*. McGraw-Hill New York. pp 10
24. Pouclet A, Wandji P, Ruffet G, Dongmo AK, Tagheu PC, et al. (2014) The mount Manengouba, a complex volcano of the cameroon line: volcanic history, petrological and geochemical features. *J Afri Earth Sci*, 97:297–321
25. Marzoli A, Renne PR, Piccirillo EM, Castorina F, Bellieni G, Melfi AJ, Nyobe JB, N'ni J. (1999) Silicic magmas from the continental Cameroon volcanic line (Oku, Bamouto and Ngaoundere): <sup>40</sup>Ar/<sup>39</sup>Ar dates, petrology, Sr–Nd–O isotopes and their petrogenetic significance. *Contribut Mineral Petrol* 135:133–150
26. Dumort JC (1968) *Carte Géologique De Reconnaissance De La République Fédérale Du Cameroun Feuille NC: NB 32 SE 028*, Par la Direction des Mines et de la Géologie, C ESPINASSE BRGM Société Nouvelle de Cartographies Lith. Paris
27. Neba A (1999) *Modern geography of the republic of cameroon*, 3rd edn. Neba Publishers, Bamenda, Cameroon
28. Molua, EL, Lambie CM (2001) *Climate, hydrology and Water Resources in Cameroon*. Environmental Issues: Problems and Prospects, Bamenda: Unique Printers, 45–66.
29. Maune DF, Amar N (2019) *Digital Elevation Model Technologies and Applications*. The DEM User's Manual, 3rd ed; Asprs Publications: Falls Church, VI, USA.
30. Zhou Q, Liu X (2004) Error analysis on grid-based slope and aspect algorithms: computer science. *Photogram Eng Remote Sens*. <https://doi.org/10.14358/PERS.70.8.957>, CorpusID:13492272
31. Aba-Fernández MV, Ariza-López FJ, Jiménez-Gamero MD (2021) A new approach to the quality control of slope and aspect classes derived from digital elevation models. *Remote Sensing* 13:2069. <https://doi.org/10.3390/rs13112069>
32. Kocal A, Duzgun HS, Karpuz C (2004) Discontinuity mapping with automatic lineament extraction from high resolution satellite imagery; mathematics, environmental science,
33. Chanlantica S (2018) *Methodological Validation for Automated Lineament Extraction by LINE Method in PCI Geomatica and MATLAB based Hough Transformation*. *Geolog Soc Ind* 92:321–328
34. Akter A, Uddin AMH, Wahid KB, Ahmed S (2020) (2020) Predicting groundwater recharge potential zones using geospatial

- technique. *Sustain Water Res Manag* 6:24. <https://doi.org/10.1007/s40899-020-00384-w>
35. Saaty TL (2004) Fundamentals of the analytic network process—multiple networks with benefits, costs, opportunities and risks. *J Syst Sci Syst Eng* 13(3):348–379. <https://doi.org/10.1007/s11518-006-0171-1>
  36. Saaty TL (2008) Decision making with the analytic hierarchy process. *Int. J. Serv. Sci.* 1:83–98. <https://doi.org/10.1504/IJSSCI.2008.017590>
  37. Arshad A., Zhang Z., Zhang W., Dilawar A. (2020) Mapping favorable groundwater potential recharge zones using a GIS-based analytical hierarchical process and probability frequency ratio model: A case study from an agro-urban region of Pakistan (2020) *Geoscience Frontiers* 11:1805–1819
  39. Callahan J. T., Choi S. H. (1973) Development of water from fractured crystalline rocks, Republic of Korea. *Proc. 2nd Intern. Symp. Ground Water*. Palermo. Ente Sviluppo Agricola in Sicilia, pp. 299–316.
  40. Larsson L. (1981) Ground water investigations in a granite area of Sardinia, Italy. Report by UNESCO, Reg. Office for Science and Technology for South and Central Asia, New Delhi. pp. 17–25.
  41. UNESCO (1984) Groundwater in Hardrocks. Project 8.6 of the International Hydrological Programme. Imprimerie de la Manutention, Mayenne ISBN 92-3-101980-5
  42. Halliday AN, Davidson JP, Holden P, Dewolf C, Lee DC, Fitton JG (1990) Trace element fractionation in plumes and the origin of HIMU mantle beneath the Cameroon Line. *Nature* 347:523–528
  43. Halliday AN, Dickin AP, Fallick AE, Fitton JG (1988) Mantle dynamics: A Nd, Sr, Pb and O isotopic study of the Cameroon line volcanic chain. *J. Petrol.* 29:181–211
  44. Marzoli A., Piccirillo E. M., Renne P. R., Bellieni G., Iacumin M., Nyobe J. B. and Tongwa A. T. (2000) The Cameroon Volcanic Line Revisited: Petrogenesis of Continental Basaltic Magmas from Lithospheric and Asthenospheric Mantle Sources. *Journal OF Petrology* Vol 41 Number 1.
  45. Gountié Dedzo M, Njonfang E, Nono A, Kamgang P, Zangmo Tefougoum G, Kagou Dongmo A, Nkouathio DG (2012) Dynamic and evolution of the Mounts Bamboutos and Bamenda calderas by study of ignimbritic deposits (West-Cameroon, Cameroon Line). *Syllabus Review. Sci. Ser.* 3:11–23
  46. Keleko TDA, Tadjou JM, Kamguia J, Tabod CT, Feumoe ANS, Kenfack JV (2013) Groundwater Investigation Using Geoelectrical Method: A Case Study of the Western Region of Cameroon. *Journal of Water Resource and Protection* 5:633–641
  47. Ngako KD, Kenfack JV, Pelap FB, Deumanou Messe M, R. (2021) Structural analysis of Haut-Nkam division, Central-Africa using remote sensing data and GIS technics. *The Egyptian Journal of Remote Sensing and Space Sciences.* <https://doi.org/10.1016/j.ejrs.2021.06.008>
  48. Elsheikh AA, Gao SS, Liu KH (2014) Formation of the Cameroon Volcanic Line by lithospheric basal erosion: Insight from mantle seismic anisotropy. *Journal of African Earth Sciences* 100:96–108
  49. Chenyi MLV, Nkouathio DG, Wotchoko P, Kouankap Nono G, D., Zénon I., Guedjeo C. S. and Tchokona Seuwei D. (2017) Volcanology and geochemical study of the volcanic rocks of the Bafmeng area (Mount Oku, Cameroon Volcanic Line). *Int. J. Biol. Chem. Sci.* 11(2):841–864
  50. Krishnamurthy J, Mani A, Jayaraman V, Manivel M (2000) Groundwater resources development in hard rock terrain—an approach using remote sensing and GIS techniques. *Int J Applied Earth Observation Geoinformation* 2(3–4):204–215
  51. Magesh NS, Chandrasekar N, Soundranayagam JP (2011) Morphometric evaluation of Papanasam and Manimuthar watersheds, parts of Western Ghats, Tirunelveli district, Tamil Nadu India: a GIS approach. *Environmental Earth Science* 64:373–381
  52. Magesh NS, Chandrasekar N, Vetha Roy D (2011) Spatial analysis of trace element contamination in sediments of Tamiraparani estuary, southeast coast of India. *Estuarine, Coastal and Shelf Science* 92:618–628
  53. Gouri SB (2020) An approach to demarcate groundwater recharge potential zone using geospatial technology. *Applied Water Science* 10:138. <https://doi.org/10.1007/s13201-020-01231-1>

**Publisher's Note** Springer Nature remains neutral with regard to jurisdictional claims in published maps and institutional affiliations.